13th ewtec 2019 Proceedings of the 13th European Wave and Tidal Energy Conference 1-6 Sept 2019, Naples, Italy

Influence of turbulence and wave flow conditions on different scaled tidal turbines

Grégory Pinon, Charifa El Hadi, Myriam Slama, José Nuño, Pablo Mansilla, Erwann Nicolas, Julie Marcille, Jean-Valéry Facq, Inès Belarbi, Benoît Gaurier, Grégory Germain, André Pacheco, and Michael Togneri

***Abstract*—In the framework of the MONITOR project, a collaborative multi-model investigation of Tidal Energy Converter (TEC) blade reliability is proposed. The global objectives of the MONITOR project is to investigate TEC reliability for converters subjected to real in-situ flow conditions, which can present high ambient turbulence and severe wave conditions. This paper will focus on the laboratory testings that were carried out at the IFREMER flume tank, on scaled models of the floating turbine of Magallanes Renovables and the bottom mounted turbine of Sabella. During the trials, their performance and load fluctuations were studied for two turbulence conditions and several incoming velocities. A regular wave case was also considered. Velocity measurements were performed using a 2D Laser Doppler Velocimeter and an Acoustic Doppler Velocimeter. The loads were measured with a thrust and torque sensor. The results for the torque and thrust coefficients and their fluctuations presented in this paper are non-dimensionalised in order to ensure confidentiality. The mean dimensionless power and thrust coefficients of both scaled models are compared to those of the IFREMER turbine, showing no major differences. With respect to the fluctuating loads, and based on the presented results, the ambient turbulence intensity have a larger influence than solidity, blade profile or even blade number.**

***Index Terms*—Marine Current Turbine, Performance, wave-current loads, Turbulence, Experiment, Tidal Turbine, Power, Flume tank, Hydrodynamics**

I. Introduction

TIDAL energy constitutes an interesting resource for European countries in the Atlantic area and several concepts were proposed during the last decades. However, the development of this sector is still limited due to uncertainty in the engineering design. Hence, these technologies are still too expensive and risky to attract financial investment. In this context, the MONITOR project [1], supported by the Interreg Atlantic Area programme, was launched in 2018. Its global objectives are to investigate, using multiple testing methodologies (numerical, laboratory and at-sea), the reliability of tidal energy converters (TEC) subjected to real in-situ flow conditions (possibly with high ambient turbulence [2]–[5] and severe wave conditions [6]–[8]) and to develop tools to help TEC developers improve device reliability [9]. Particularly, two tidal energy technologies, Magallanes Renovables and Sabella turbines, are used as test subjects in the investigation.

The present study will concentrate on the experimental investigations carried out by the University of Le Havre Normandy and the IFREMER (French Research Institute for Exploitation of the Sea) Boulogne-Sur-Mer, at the end of May and in early November 2018. It deals with the characterization of fluctuating loads for a single turbine immersed in a regular current flow (with different levels of turbulence) and a combined wave and current configuration. During these trials, scaled models of both Magallanes and Sabella turbines were tested and compared to the IFREMER turbine [10]–[13]. In this paper, we present the results obtained for two turbulence intensities (1.3% and 15%) without wave and for one regular wave case. Several incoming velocities were also considered. The scaled tidal turbines and the experimental set-up are described in the following section. The analysis of the torque and thrust coefficients, together with their fluctuations, is presented in Section III.

II. Experimental set-up

In this section, the turbine models as well as the flume tank and the instrumentation are described. The different flow and wave conditions considered are also presented.

A. Turbine models description

The turbine scaled models are based on pre-commercial prototypes, namely the floating Magallanes Renovables turbine and the bottom mounted Sabella turbine.

The turbine of Magallanes Renovables (Fig. 1) is a floating device composed of a 3-bladed bi-rotor turbine. The turbine diameter is $D = 19$ m, its overall length is 45 m, its breadth is 6 m and its weight is 350 tons. The turbine is designed for a maximum power output of 2 MW. Its platform is anchored to

The ID number of this paper is 1495 of the conference track TDD: Tidal Device Development and Testing. This project is co-financed by the European Regional Development Fund through the Interreg Atlantic Area Programme, via the MONITOR project. This work was also supported in part by the European ERDF and Normandy Regional Funding program NEPTUNE. This work benefits from studies carried out within the framework of H2020 MaRINET2 Round Robin tests and the Interreg 2 Seas MET-CERTIFIED project.

G. Pinon, C. El Hadi and M. Slama are with Normandie Univ, UNIHAVRE, UMR 6294 CNRS, LOMC 76600 Le Havre, France (e-mail: gregory.pinon@univ-lehavre.fr).

J. Nuño and P. Mansilla are at Magallanes Renovables, Prego de Montaos 7, Redondela, Spain, 36800.

E. Nicolas and J. Marcille are at Sabella S.A.S., 11 Rue Félix Le Dantec, 29000 Quimper, France.

J.-V. Facq, I. Belarbi, B. Gaurier and G. Germain are at the IFREMER, 150 Quai Gambetta, 62200 Boulogne s/ Mer, France.

A. Pacheco is with CIMA, University of Algarve Edificio 7, Campus de Gambelas, 8005-139 Faro, Portugal.

M. Togneri is with Marine Energy Research Group, Swansea University, Bay Campus, Swansea SA1 8EN, UK.

TABLE I
FROUDE SCALING CHARACTERISTIC BETWEEN THE PROTOTYPE SCALE AND THE MODEL SCALE FOR EACH TURBINE.

Turbine physical parameters	Froude Scaling	Magallanes Scale 1 : 1	Magallanes Scale 1 : 28	Sabella Scale 1 : 1	Sabella Scale 1 : 20	IFREMER -
Radius R (m)	$1:\lambda$	9.5	0.338	6	0.300	0.362
Water depth H (m)	$1:\lambda$	56*	2	40*	2	2
Flow speed (m/s)	$1:\sqrt{\lambda}$	$[4.2-7.4]$	$[0.8-1.4]$	$[3.6-6.3]$	$[0.8-1.4]$	$[0.8-1.2]$
TSR range (-)	-	$[0-8]$	$[0-8]$	$[0-6]$	$[0-6]$	$[0-8]$
Reynolds Re_∞ (-)	$1:\lambda\sqrt{\lambda}$	$[4.0-7.0]\times10^7$	$[2.7-4.7]\times10^5$	$[2.2-3.8]\times10^7$	$[2.4-4.2]\times10^5$	$[2.9-4.3]\times10^5$

The chosen Froude scaling range is $Fr_\infty = [0.18-0.32]$ for the three scaled turbines depending on the considered velocity.
* Hypothetical water depth based on the scale factor.

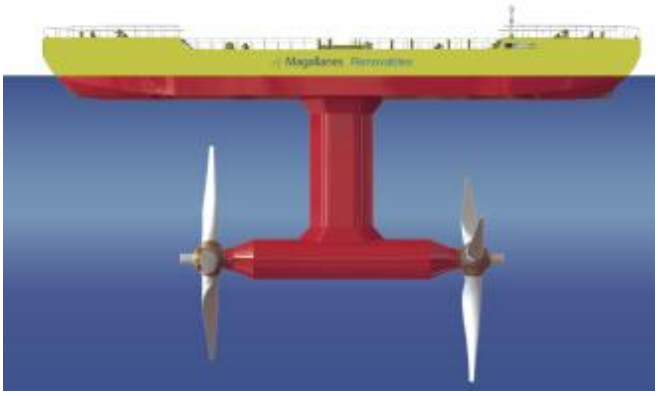

Fig. 1. Schematic CAD representation of the turbine of Magallanes Renovables.

the sea bottom by four mooring lines, to the bow and stern. A first full scale prototype was deployed at the European Marine Energy Centre (EMEC), Scotland, during summer 2018.

Fig. 2. D10 SABELLA turbine on the port of Brest before immersion in the Fromveur Strait, near Ushant Island in Sept. 2015.

The other model is a scaled model of the Sabella D12 turbine. The tested turbine is a new version of the existing Sabella D10 turbine (with 6 blades), already immersed in the Fromveur Strait, France (Fig. 2). As a matter of information, the D10 had a total height of 17 m from the seabed and its weight was 400 tons with a gravity based support structure. The D10 is designed for a maximum power output of 1 MW at a current velocity of 4 m/s. The new D12 tested technology is composed of a single rotor with 5 fixed (no-pitch) and symmetrical blades. This kind of turbine can be installed in open sea areas (possibly swept by waves), where tidal currents exceed 1.75 m/s, with depths of 25 to 50 meters.

And finally, results from the open-geometry scaled turbine of IFREMER [10]–[13] will also be used as a matter of comparison. Therefore, there is a total of 3 different turbines at similar model scales that were tested for the same inflow conditions with the same test facility and instrumentation. Pictures of each of the three scaled turbines used in these trials are depicted in Figure 3.

The scaling parameters chosen for both pre-commercial turbines are presented in Table I. As in many other similar studies, a Froude scaling was applied to scale the blade length, the water depth, the flow velocity, the rotational speed, etc. The Froude number is defined as:

$$Fr_\infty = \frac{U_\infty}{\sqrt{g \times H}}, \tag{1}$$

where $g = 9.81$ m/s^2 is the gravitational acceleration, H is the flume tank depth and U_∞ is the upstream velocity. The corresponding Reynolds numbers, defined as:

$$Re_\infty = \frac{U_\infty \times R}{\nu} \tag{2}$$

(where ν is the kinematic viscosity of the fluid), are also given in Table I as a matter of information.

TABLE II
TURBINE MODEL PARAMETER DESCRIPTION.

Description	IFREMER	Magallanes	Sabella
Profile	NACA 63418	-	-
Rotor Radius R (mm)	362	338	300
Hub Radius (mm)	55	55	96
Hub length (mm)	720	720	720
Number of blades	3	3	5
Blade length (mm)	307	283	204
Direction of rotation	C	CC	C

C: clockwise; CC: counter-clockwise.

Both Magallanes and Sabella scaled turbines, shown in Fig. 3, are in fact based on the existing IFREMER

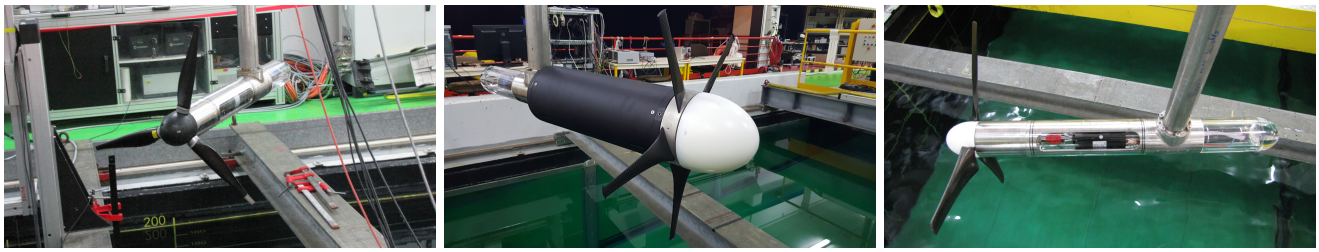

Fig. 3. Pictures of the scaled turbine models: left is Magallanes Renovables, middle Sabella, and right is IFREMER.

generic turbine, a tri-bladed turbine with a horizontal axis, used in previous works [11], [13]. Only the blades, the hub and the careenage for the nacelle were changed to adapt the turbine to the industrial device geometries. Model parameters, such as the hub radius and the blade lengths, are detailed in Table II. The blades of the IFREMER turbine are designed from a NACA 63418 profile. Magallanes and Sabella blade profiles are confidential.

The rotor is connected to a motor-gearbox assembly consisting of a gearbox, a DC motor, a ballast load and a motor speed control unit [2], [12], providing an active rotor speed control. The pitch of the blade is fixed to 0 degree in each case.

The Tip Speed Ratio (TSR) is defined as the ratio of the tip velocity of the blade to the upstream flow velocity:

$$TSR = \frac{\omega_x \times R}{U_\infty} \tag{3}$$

where ω_x is the axial rotation speed. Although not studied here, the influence of the rotational speed ω_x fluctuations on the performance fluctuations will need to be evaluated in a near future. In this study, the TSR varies from 0 to 8 for the Magallanes model and from 0 to 6 for the Sabella turbine.

B. Flume tank description and experiment configurations

The tests of the scaled turbines were carried out in the IFREMER wave and current flume tank in Boulogne-sur-mer. It is the same infrastructure as the one used in the previous work of [2], [3], [14], [15] or more recently [12]. The experimental set-up, illustrated in Fig. 4 and Fig. 5, is mainly made up of the turbine model, a 2D Laser Doppler Velocimeter (LDV) and an Acoustic Doppler Velocimeter (ADV). A side view of the LDV and the ADV systems is presented in Fig. 6. Three wave probes are also used to measure the wave characteristics.

The torque and thrust are directly measured on the rotation axis. To evaluate the performance of both models, we used the power and thrust coefficients which are defined respectively by:

$$C_P = \frac{Q \times \omega_x}{\frac{1}{2}\rho S U_\infty^3} \tag{4}$$

and :

$$C_T = \frac{T}{\frac{1}{2}\rho S U_\infty^2} \tag{5}$$

where Q is the torque, T is the thrust and ρ is the fluid density.

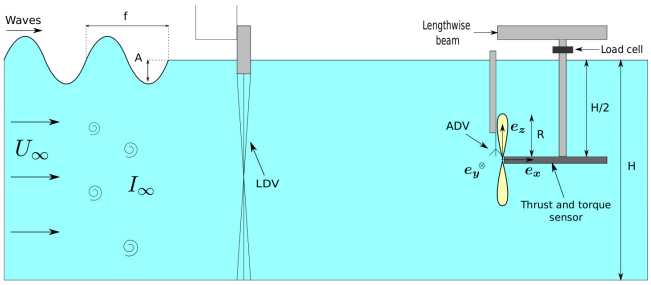

Fig. 4. Schematic side-view of the turbine configuration equivalent to the picture presented in Fig. 5. The origin $O(0,0,0)$ is chosen at the rotor centre.

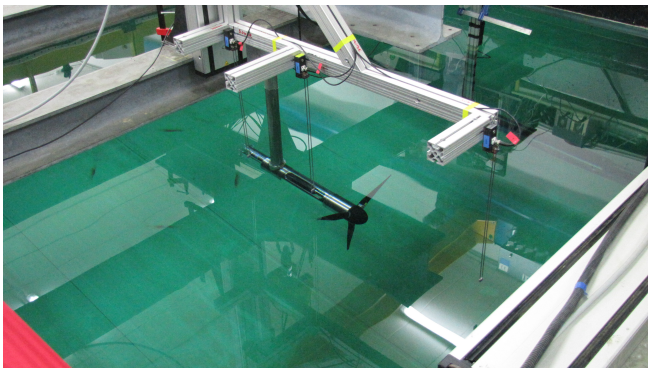

Fig. 5. Top view of the assembly with the three wave gauges.

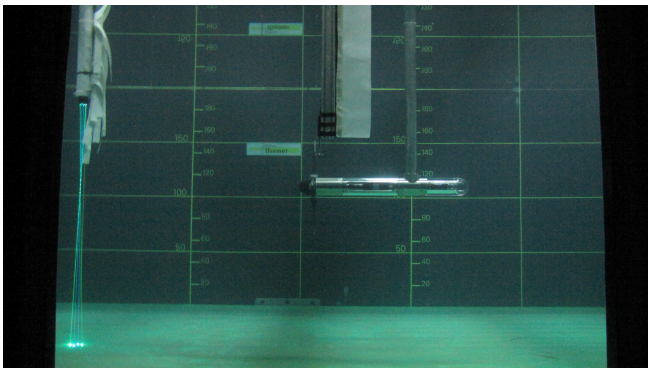

Fig. 6. Side view of the turbine in the flume tank with the 2D LDV (left) and the ADV systems.

The flume tank is $L = 18$ m long, $\ell = 4$ m wide and $H = 2$ m deep as presented in Fig. 7. The blockage ratio α is defined as the ratio between the rotor cross-section area $S = \pi \times R^2$ and the flume tank transverse area $A = l \times H$:

$$\alpha = \frac{S}{A} = \frac{\pi \times R^2}{l \times H}. \tag{6}$$

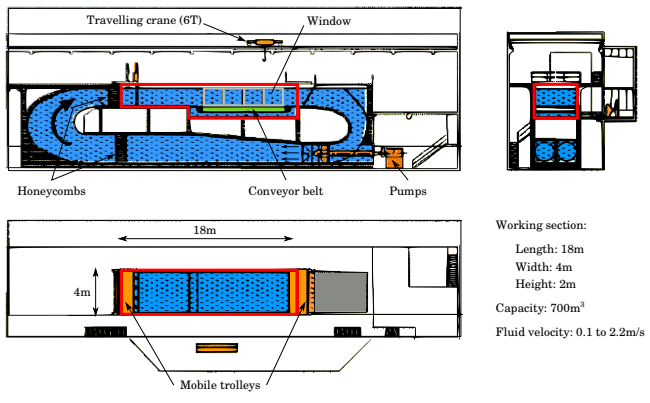

Fig. 7. IFREMER's Boulogne-sur-Mer flume tank.

The blockage ratios for these trials are $\alpha \approx 4.5\%$ and $\alpha \approx 3.5\%$ for Magallanes and Sabella scaled turbines respectively. For the IFREMER model, this ratio is about 5.1%. In this study we used a range of upstream velocity going from $U_\infty = 0.80$ m/s to $U_\infty = 1.4$ m/s. This corresponds to a full scale velocity range of 4.2-7.4 m/s for the Magallanes turbine and 3.6-6.3 m/s for the Sabella turbine (see Table I). In energetic sites (*e.g* Alderney race, Fromveur strait, Fall of Warness, Bay of Fundy, etc.), velocities at the order of 5 m/s are regularly obtained. Even higher velocities could be encountered for the highest tidal coefficients, which are not so frequent. Therefore, the velocity range studied here is relevant for the higher velocities encountered in highly energetic sites. The ambient turbulence I_∞ generated in the flow can be regulated using flow straighteners: it goes from $I_\infty = 1.3\%$ when both a grid and honeycombs are used, to $I_\infty = 5\%$ when only the honeycombs are used and to a higher value of $I_\infty = 15\%$ when removing all the flow straighteners. In the present study only $I_\infty = 1.3\%$ and $I_\infty = 15\%$ were used. I_∞ is here defined as:

$$I_\infty = 100\sqrt{\frac{1/3(\sigma^2(u_\infty) + \sigma^2(v_\infty) + \sigma^2(w_\infty))}{\overline{u}_\infty^2 + \overline{v}_\infty^2 + \overline{w}_\infty^2}} \qquad (7)$$

with $\sigma(u_\infty)$, $\sigma(v_\infty)$ and $\sigma(w_\infty)$, the standard deviations of the velocity components u_∞, v_∞ and w_∞ of the upstream velocity $\boldsymbol{u}_\infty$. The overbar denotes the time average. The I_∞ range used in this study corresponds to measured in-situ values [2], [4], [5], [16] and generally used for experimental studies [15].

C. Wave characteristics

In addition to the cases described above, the turbine models were also tested with several wave conditions, for $U_\infty = 1.0$ m/s and with the same flow straighteners as for the *current only* case with $I_\infty = 1.3\%$. A piston-type wave generator was used to generate regular waves at the upstream end of the flume tank [17]. The selected period range from 1.43 s to 2 s at model scale, corresponding to prototype periods going from 6.4 s to 10.6 s. For the wave amplitude, we took 2 different values, 0.095 m and 0.130 m, in order to adapt the operation of the turbine. An additional case with the wave generator immersed without functioning (referred to as *wavemaker only*) was also performed to have a baseline configuration with the presence of the wavemaker and thus a specific vertical velocity profile. Finally, cases with irregular waves and some other regular wave conditions, were also performed but not presented in the present paper.

TABLE III
MODELLED OFFSHORE WAVE CONDITIONS FOR THE EMEC TIDAL TEST SITE (SCOTLAND).

Return period (years)	1	5	10	25	50	100
Significant wave height Hm_0 (m)	4.3	5	5.3	5.7	6	6.3
Peak wave period Tp (s)	8.5	9.2	9.4	9.8	10.1	10.3

TABLE IV
THE WAVE CONDITIONS APPLIED IN THE *MONITOR* PROJECT.

Amplitude (m)	0.095	0.130
Frequency (Hz)	0.5	0.7
Period (s)	2	1.43
Full scale wave height (m)	≈3.8-5.3	≈5.2-7.3
Full scale period (s)	≈8.9-10.6	≈6.4-7.6

Taking into account on-site data from the EMEC [18], Table III presents the significant wave height Hm_0 obtained by hindcast simulation for different return periods. Although not completely detailed on the cited reference [18], it is assumed that these results are obtained on the whole dataset. These wave conditions can be compared to those used in the *MONITOR* project and presented in Table IV. In fact, Table IV presents the wave conditions at model scale used during the trials in terms of wave amplitude, frequency and period. From these parameters, corresponding full scale wave heights of $H = 5.3$ m and 7.3 m can be obtained for the 1:28 scale with the Magallanes turbine, itself deployed at EMEC. Lower values are then obtained for the configuration at a scale of 1:20 (Sabella) and reproduced in Table IV. The *MONITOR* wave conditions therefore correspond to full scale conditions possibly encountered at Fall of Warness, were the Magallanes turbine is deployed. However, these previous information need to be taken with caution. In fact, more precise information are needed in order to ascertain the likelihood of such wave conditions with the studied upstream velocity. Additionally, the presented results with waves are very preliminary and forthcoming analysis will improve their quality very shortly.

III. PERFORMANCE EVALUATION

The results obtained for the mean power and thrust coefficients and their standard deviations, as a function of the TSR, are presented in this section. The values were averaged over a time of 180 s to 360 s, according to the *current and wave* conditions, in order to be fully converged. As the blade profiles for both turbines are confidential, all results were divided by a coefficient:

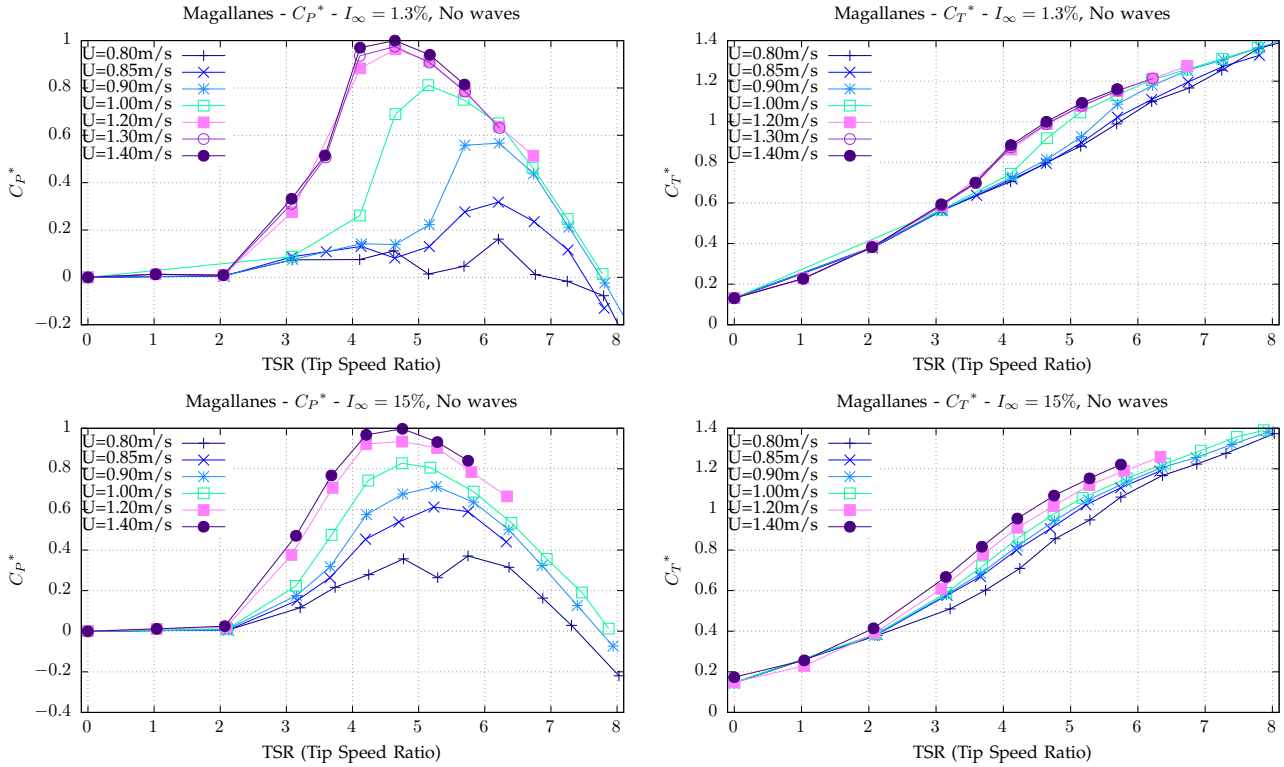

Fig. 8. Adimensional power and thrust coefficients for the two ambient turbulence intensity cases, namely $I_\infty = 1.3\%$ and $I_\infty = 15\%$.

- power coefficients and their standard deviations are divided by the maximum C_P value at $U_\infty = 1.4$ m/s and $I_\infty = 1.3\%$.
- thrust coefficients and their standard deviations are divided by the C_T value at the TSR of the maximum value of C_P (at $U_\infty = 1.4$ m/s and $I_\infty = 1.3\%$).

The adimensional values will be identified by $*$. However a qualitative comparison of the two technologies is still possible and is presented at the end of this section.

D. Magallanes turbine

1) Power and thrust coefficients without wave: Fig. 8 shows the power and thrust coefficients obtained for several upstream velocities and the two considered ambient turbulence intensities ($I_\infty = 1.3\%$ and $I_\infty = 15\%$). For both turbulence intensities, the Magallanes turbine operates properly for upstream velocities above 1.2 m/s. For these velocities the $C_P{}^*$ curves tend to collapse into a single curve over the whole TSR range. For the lower upstream velocities ($U_\infty \leq 1.0$ m/s), an important Reynolds effect is observed. This Reynolds effect is mainly observable at the laboratory scale (see Table I) but for the lower velocities (*e.g.* $U_\infty \leq 0.85$ m/s), the turbine hardly operates for the lower turbulence intensity. As expected, this Reynolds effect is largely attenuated for the higher turbulence intensity and the shape of the performance curves are improved for $I_\infty = 15\%$. For both I_∞ configurations, the operating range is similar and comprised in $4 \leq TSR \leq 5.5$, but it has a slightly narrowed tendency for the lower ambient turbulence case. For both ambient turbulence configurations and for velocities ≥ 1.2 m/s, the maximal $C_P{}^*$ value is reached.

Very similar behaviour are observed for the thrust coefficients. Again a Reynolds effect is visible, although less important, for upstream velocities lower than 1.2 m/s for $I_\infty = 1.3\%$. But beyond this velocity, the thrust coefficient curves are also superimposed. On the contrary, at $I_\infty = 15\%$ the curves do not superimpose. For both turbulence intensities, the thrust coefficient keeps increasing with the TSR value. This observation differs slightly from the results of [2] but is very similar to the recent results of Gaurier *et al.* [12].

2) Power and thrust coefficients in case of current and wave*:* The power and thrust coefficients were also computed for a case with *current and wave*. In the present paper, only a single configuration with a wave amplitude $A = 0.095$ m and a frequency $f = 0.5$ Hz is presented. As a matter of comparison, the turbine was tested with the wave generator immersed without any movement. This last case is referred to as *Wavemaker only* in the graphs. The performance curves, presented in Fig. 9, have similar maximum values but the $C_P{}^*$ curves are different. This is not what is usually found in the literature, where the mean C_P (*resp.* C_T) curves superimpose with and without wave. Additionally, in recirculating tank, the wavemaker modifies the velocity profile [13] and hence the mean incoming velocity. With the important Reynolds dependence of the scaled Magallanes turbine, additional care should be taken for this configuration with wave. These aspects will be treated more into detail in the upcoming analysis.

3) Standard deviation: Fig. 10 depicts the standard deviations of the power and thrust coefficients, $\sigma_{C_P{}^*}$ and $\sigma_{C_T{}^*}$. When the turbine is operating with a velocity lower than $U_\infty = 1.2$ m/s, meaning that the Reynolds effect is still very important, these quantities

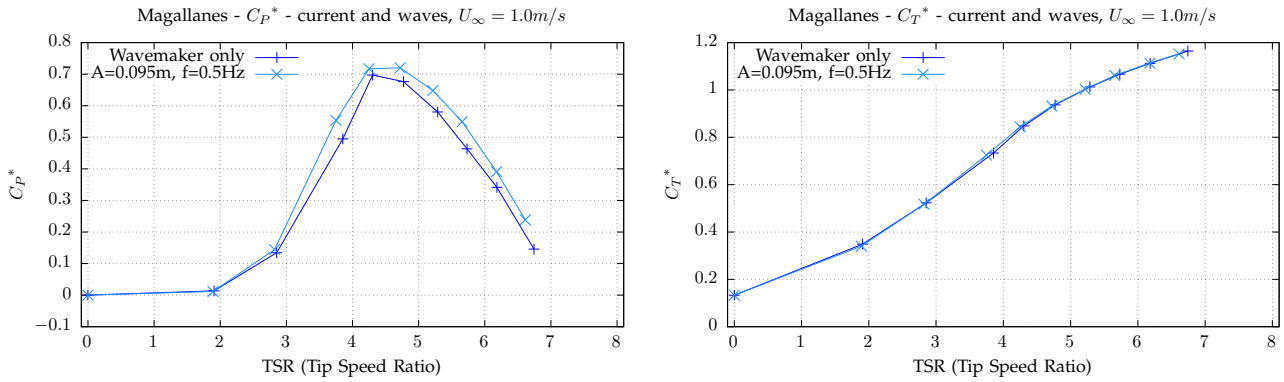

Fig. 9. Adimensional power and thrust coefficients, for a current velocity $U_\infty = 1.0$ m/s, in case of combined *current and wave*.

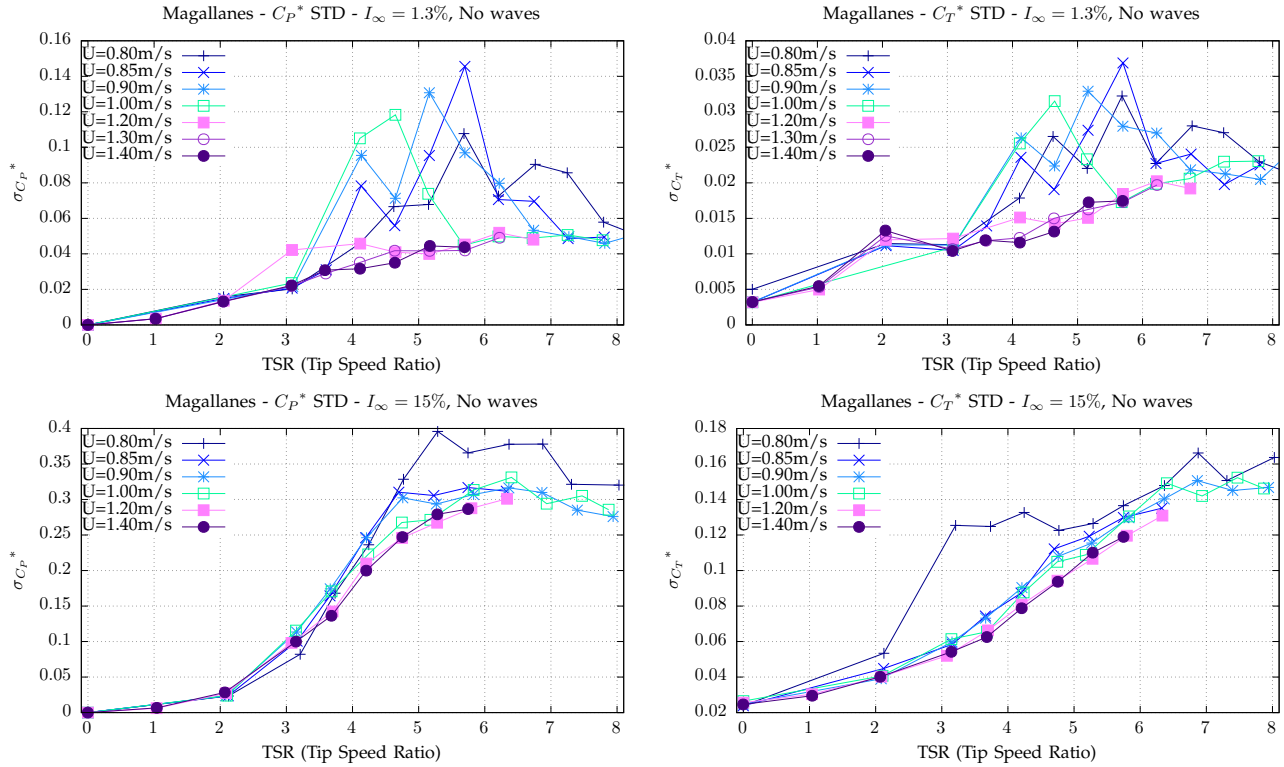

Fig. 10. Adimensional standard deviation of the power and thrust coefficients for the two ambient turbulence intensity cases, namely $I_\infty = 1.3\%$ and $I_\infty = 15\%$.

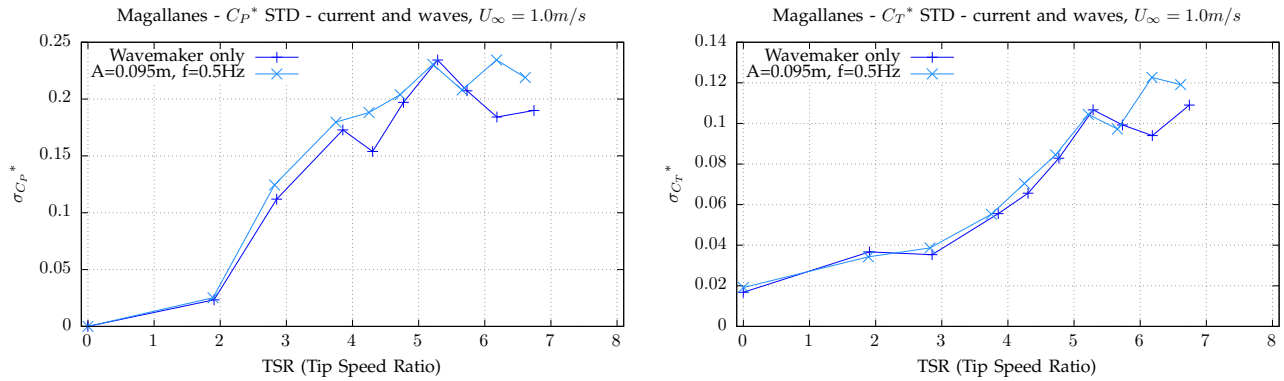

Fig. 11. Adimensional standard deviation of the power and thrust coefficients, for a current velocity $U_\infty = 1.0$ m/s, in case of combined *current and wave*.

are doubled (for $\sigma_{C_T{}^*}$) to tripled (for $\sigma_{C_P{}^*}$) to the corresponding values for the higher upstream velocities. This means that important "dynamic stall" or similar unsteady hydrodynamics features are present

at some location of the blade due to this Reynolds effect. But apart from that, for the higher incoming velocities (*e.g* $U_\infty \geq 1.2$ m/s), the turbulence intensity has an important influence on ${\sigma_{C_P}}^*$ and ${\sigma_{C_T}}^*$. Indeed, for those velocities and at the operating range of TSR ($4 \leq TSR \leq 5.5$), the ${\sigma_{C_P}}^*$ increase from ≈ 0.04 with $I_\infty = 1.3\%$ to ≈ 0.25 with $I_\infty = 15\%$ corresponding to approximately a multiplication by 6. And a multiplication by approximately 8 or 9 is observed for the ${\sigma_{C_T}}^*$; with values going from $\approx 0.012 - 0.015$ with $I_\infty = 1.3\%$ to $\approx 0.08 - 0.11$ with $I_\infty = 15\%$. The turbine response in terms of standard deviation of ${C_P}^*$ and ${C_T}^*$ in the case of combined wave and current conditions is quite similar to the case of $I_\infty = 15\%$ (see Fig. 11). This unpredicted result need to be further analysed. In fact, the presence of the wave maker, even if it is not operating, increase the background level of turbulence whose intensity will need to be evaluated. Therefore, special treatment will be necessary to distinguish between the performance fluctuations due to the wavemaker-only generated turbulence and those due to the waves when the wavemaker is operating. Again, this will be the topic of the forthcoming analysis.

E. Sabella turbine

1) Power and thrust coefficients without wave: Fig. 12 shows the power and thrust coefficients obtained for the Sabella scaled turbine, for the *current only* cases. The tests were carried out at the same turbulence intensities as before and for 4 velocities ($U_\infty = 0.8$, 1.0, 1.2 and 1.4 m/s). For both turbulence intensities, the device operates without any major Reynolds influence. Whatever the upstream velocity is, the ${C_P}^*$ and ${C_T}^*$ curves quasi superimpose for both ambient turbulence intensities. Both power and thrust coefficients have similar values at $I_\infty = 1.3\%$ and $I_\infty = 15\%$, slightly lower for the later case. For a given ambient turbulence level, only a minor Reynolds effect is observable on the maximum values of power as explained in Gaurier *et al.* [10]. For this turbine, the operating range is contained in $3.75 \leq TSR \leq 5$.

2) Power and thrust coefficients in case of current and wave*:* The mean power and thrust coefficients computed in the case of *current and wave* are presented in Fig. 13. The Sabella turbine was also tested, for a fixed value of upstream velocity of $U_\infty = 1.0$ m/s, with the wave generator only and with a wave amplitude $A = 0.095$ m and a frequency $f = 0.5$ Hz. For both coefficients, the curves superimpose for the whole tested TSR range, which is limited to 3.5 for the case with a wave amplitude $A = 0.095$ m due to a failure in the wavemaker during this set of trials.

3) Standard deviation: Similarly to the case of the Magallanes turbine, the ambient turbulence intensity has an important influence on the standard deviations of ${C_P}^*$ and ${C_T}^*$ (see Fig. 14). For all velocities and for TSR $\geqslant 2$, ${\sigma_{C_P}}^*$ and ${\sigma_{C_T}}^*$ are 3 to 9 times higher with $I_\infty = 15\%$ than with $I_\infty = 1.3\%$. To be more precise, for those velocities and at the operating range of TSR ($3.75 \leq TSR \leq 5$), the ${\sigma_{C_P}}^*$ increase from ≈ 0.03 with $I_\infty = 1.3\%$ to $\approx 0.1 - 0.27$ with $I_\infty = 15\%$. And a multiplication by approximately 6 to 10 is observed for the ${\sigma_{C_T}}^*$; with values going from ≈ 0.014 with $I_\infty = 1.3\%$ to $\approx 0.09 - 0.14$ with $I_\infty = 15\%$. Besides, for $I_\infty = 15\%$, ${\sigma_{C_P}}^*$ and ${\sigma_{C_T}}^*$ curves superimpose for all velocities. In the case of *current and wave*, the standard deviations of ${C_P}^*$ and ${C_T}^*$ are similar to the results for $I_\infty = 15\%$ (see Fig. 15).

F. Comparison between the Magallanes, Sabella and the IFREMER turbines

The performances of both Magallanes and Sabella scaled turbines are now compared: for 3 velocities ($U_\infty = 0.8$, 1.0 and 1.4 m/s) in case of *current only*. These curves are compared with the existing results on the IFREMER turbine [11], [12]. It is reminded that the dimensionless values of the ${C_P}^*$ and ${C_T}^*$ are those presented at the beginning of the section III. For the new scaled IFREMER turbine, results at $U_\infty = 1.4$ m/s presently do not exist yet. As a consequence, the dimensionless procedure was performed using the maximum C_P value obtained for a velocity of $U_\infty = 1.2$ m/s. At this stage, comparison on combined *current and wave* conditions are not presented in the present paper.

1) Power and thrust coefficients: The power and thrust coefficients obtained for the three scaled turbines, for the *current only* case, are shown in Fig. 16. As expected, the power coefficient curve for the Magallanes model is close to the Sabella turbine results only for $U_\infty = 1.4$ m/s at $I_\infty = 1.3\%$. For this last inflow condition, both curves of Sabella and Magallanes are in fact very close together although the turbines have a very different design. It is however worth mentioning here that, this comparison is only valid for the dimensionless results. The IFREMER turbine presents a larger operating range ($3.0 \lesssim TSR \lesssim 5.0$) than its two industrial counterparts. For $I_\infty = 15\%$, Sabella power coefficients curves are between the Magallanes ones for $U_\infty = 1.0$ m/s and $U_\infty = 1.4$ m/s. Again, the IFREMER turbine depicts a larger TSR operation range, very similar to the one at $I_\infty = 1.3\%$. For the higher velocities, when the Reynolds effects are suppressed, the maximum of the ${C_P}^*$ coefficient is reached around the same TSR values for all turbines: 4.25 for Sabella; 4.5 for Magallanes and 4 for the IFREMER. And this result is not modified whatever the ambient turbulence is.

With the given non-dimensionalising procedure, the Sabella thrust coefficients curves are slightly higher than the Magallanes ones for TSR values below 5 and 4 at $I_\infty = 1.3\%$ and $I_\infty = 15\%$ respectively. The results obtained for the IFREMER turbines are always a little higher than the two previous ones. For the three turbines however, the ${C_T}^*$ curves are similar in shape. Some inflexions in the curves are observed for different TSR values, this will need to be analysed in a near future. Numerical computations, such as those of Togneri *et al.* [19] could be useful in that respect.

2) Standard deviation: As described before, the turbulence intensity has an important influence on the standard deviations of the power and thrust coefficients for

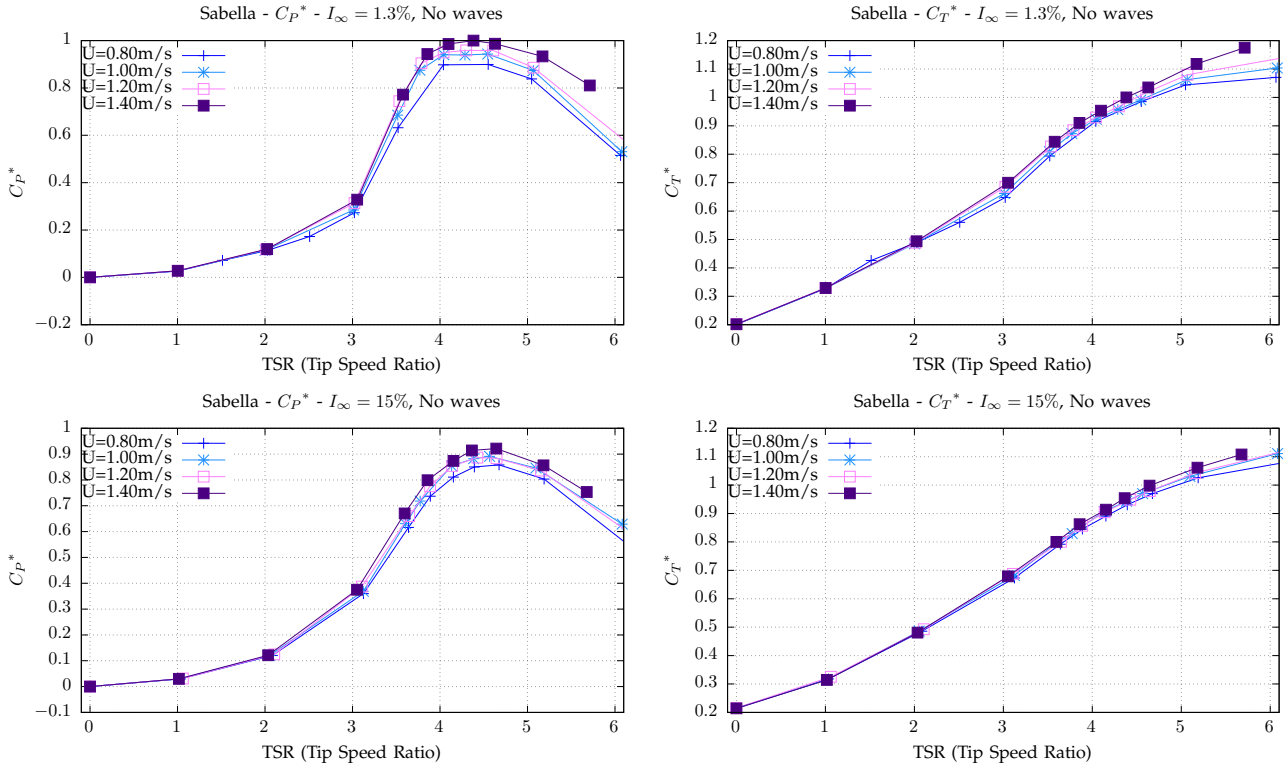

Fig. 12. Adimensional power and thrust coefficients for the two ambient turbulence intensity cases, namely $I_\infty = 1.3\%$ and $I_\infty = 15\%$.

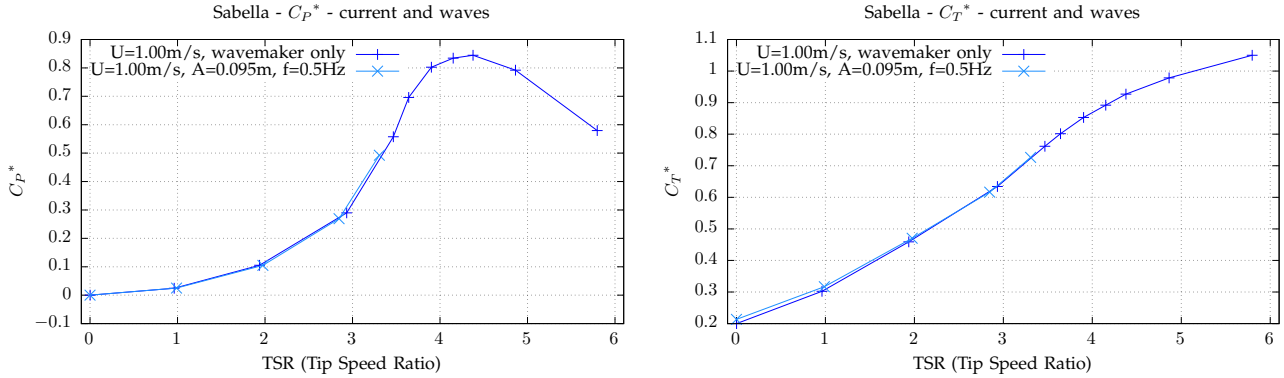

Fig. 13. Adimensional power and thrust coefficients, for a current velocity $U_\infty = 1.0$ m/s, in case of combined *current and wave*.

the three turbines (see Fig. 17). To the authors point of view, for the Magallanes turbine, the results for $U_\infty =$ 0.8 and 1.0 m/s at $I_\infty = 1.3\%$ and $U_\infty = 0.8$ m/s at $I_\infty = 15\%$ should be disregarded because the Reynolds effect may clearly affect the analysis. For the remaining curves, it is very interesting to observe that the ${\sigma_{C_P}}^*$ and ${\sigma_{C_T}}^*$ curves have similar shape and values for the three turbines.

For the lower ambient turbulence case, ${\sigma_{C_P}}^*$ values are ranging from 0.015 to ≈0.05 for the three turbines and remaining velocities. A dynamic load seems to appear at TSR =2.5 for both velocities for the IFREMER turbine. This precise aspect will need to be studied in deeper detail. For the higher ambient turbulence case, the Sabella turbine depicts lower values of ${\sigma_{C_P}}^*$ than the two other turbines. Magallanes and IFREMER turbines have very similar curves, IFREMER being only slightly higher. But for the optimal TSR value of each turbine, which lies approximately at $4.0 \lesssim TSR \lesssim 4.5$, all the three turbines have a dimensionless ${\sigma_{C_P}}^*$ of $\approx 0.20 - 0.27$.

In term of standard deviation of the thrust coefficient, again the presented dimensionless ${\sigma_{C_T}}^*$ for $I_\infty = 1.3\%$ are surprisingly all concentrated in a narrow range between 0.01 and maximum 0.02 for the operating range of TSR ($\in [3.0, 5.0]$). Analysis is still necessary on this previous assertion in order to completely ascertain this observation. For the higher ambient turbulence configuration, a tendency seems to emerge with the IFREMER turbine experiencing the higher fluctuating loads, followed by the Sabella and finally the Magallanes, still for $3.0 \lesssim TSR \lesssim 5.0$. The obtained values range from 0.06 to ≈0.14 for the higher TSR, which show an important spreading of ${C_T}^*$ fluctuations with this operating range of TSR. To conclude, this dimensionless results, observations and analyses needs to be taken with caution as absolute values may be different. However, the main

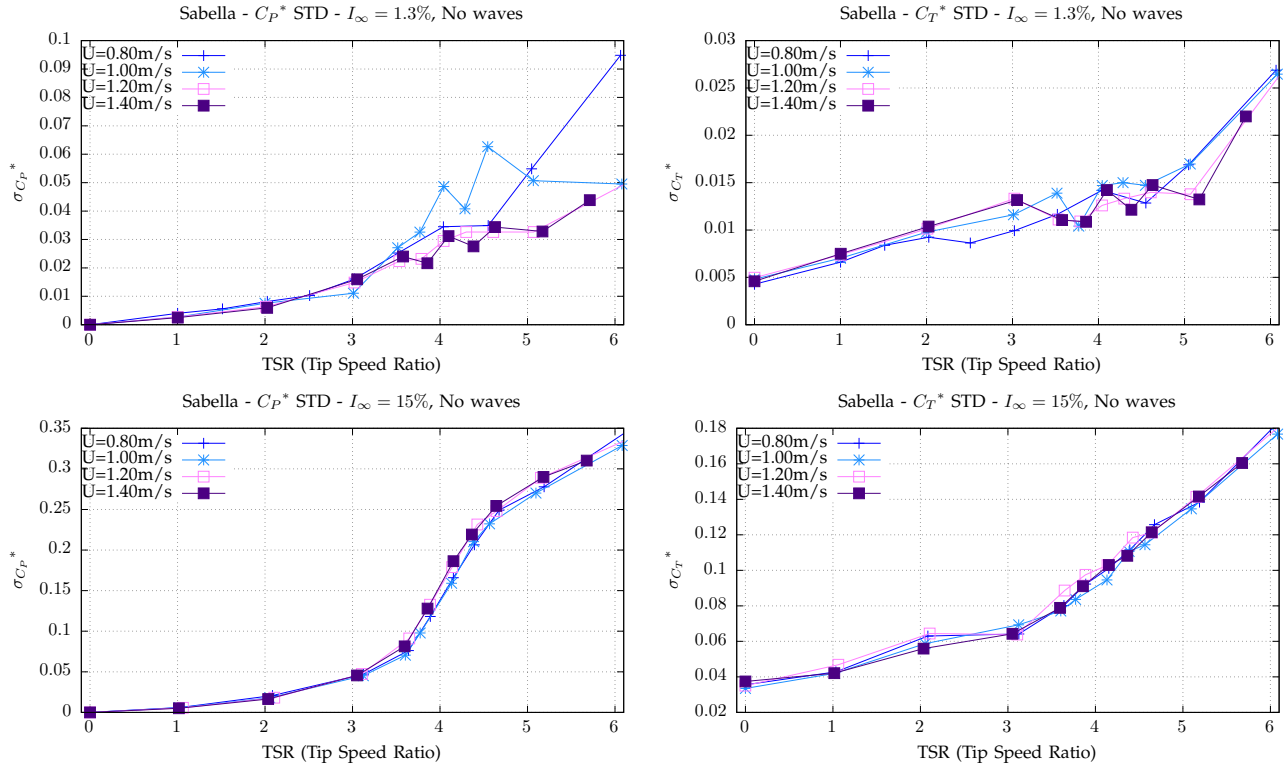

Fig. 14. Adimensional standard deviation of the power and thrust coefficients for the two ambient turbulence intensity cases, namely $I_\infty = 1.3\%$ and $I_\infty = 15\%$.

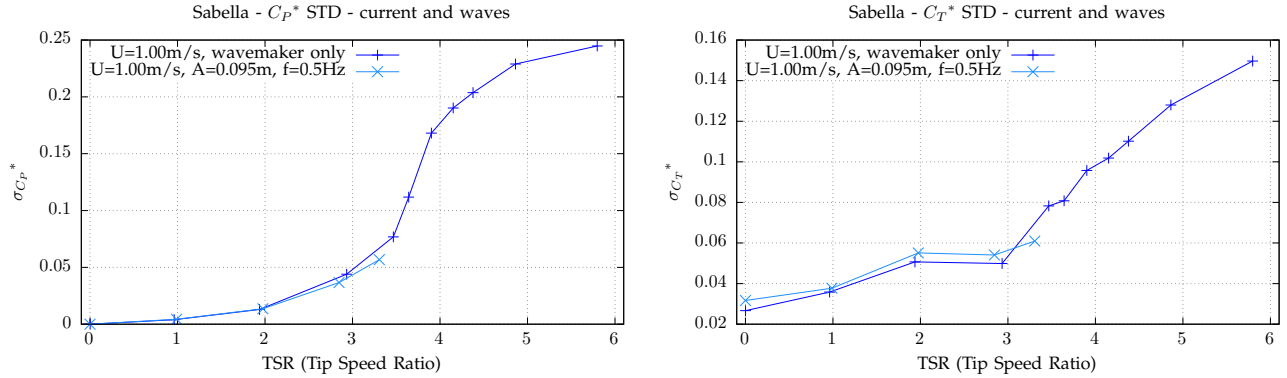

Fig. 15. Adimensional standard deviation of the power and thrust coefficients, for a current velocity $U_\infty = 1.0$ m/s, in case of combined *current and wave*.

tendencies still remain. First, ambient turbulence really have an important role on the turbine load fluctuations as already shown by Mycek *et al.* [2], Blackmore *et al.* [3] and other authors. At first glance, the turbine solidity, blade profile and blade number do not seem to have a major influence on the load fluctuations. Although the present study clearly show this assertion, this last conclusion really needs deeper studies to be comforted. One of the first contradicting possibility would be that the drive train of the IFREMER nacelle (used for all the three scaled turbine) has the larger influence on the obtained results, hiding the differences due to the rotor influence. Such conclusions would have a major influence on the fatigue of the blades and the other components of the turbines. And then, this can impact significantly the turbines design and hence their cost [20]. The whole MONITOR project will be dedicated to that aspect.

IV. Conclusions and Prospects

During this study, scale models of two industrial prototypes were tested: a 1:28 scale model of the 3-bladed horizontal axis turbine of Magallanes Renovables and a 1:20 scale model of the 5-bladed horizontal axis turbine of Sabella. The results were presented dimensionless to preserve confidentiality. These results were also compared to the open-geometry tidal turbine of IFREMER using a similar dimensionless procedure. These laboratory trials were performed using two turbulence intensities, namely $I_\infty = 1.3\%$ and $I_\infty = 15\%$ and several upstream velocities without wave. The influence of combined *current and wave* conditions was also presented for $I_\infty = 1.3\%$ and $U_\infty = 1.0$ m/s for a single regular wave case.

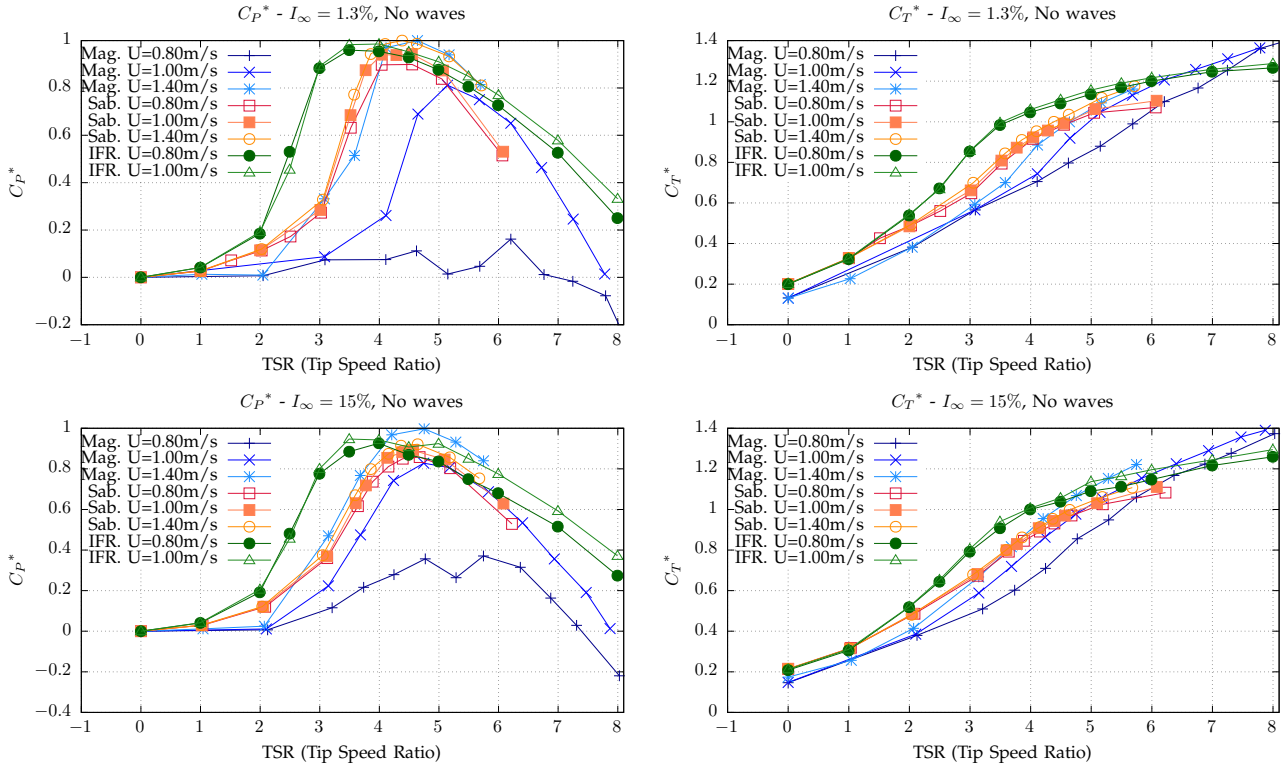

Fig. 16. Comparison of the adimensional power and thrust coefficients of Magallanes, Sabella and IFREMER turbines for the two ambient turbulence intensity cases.

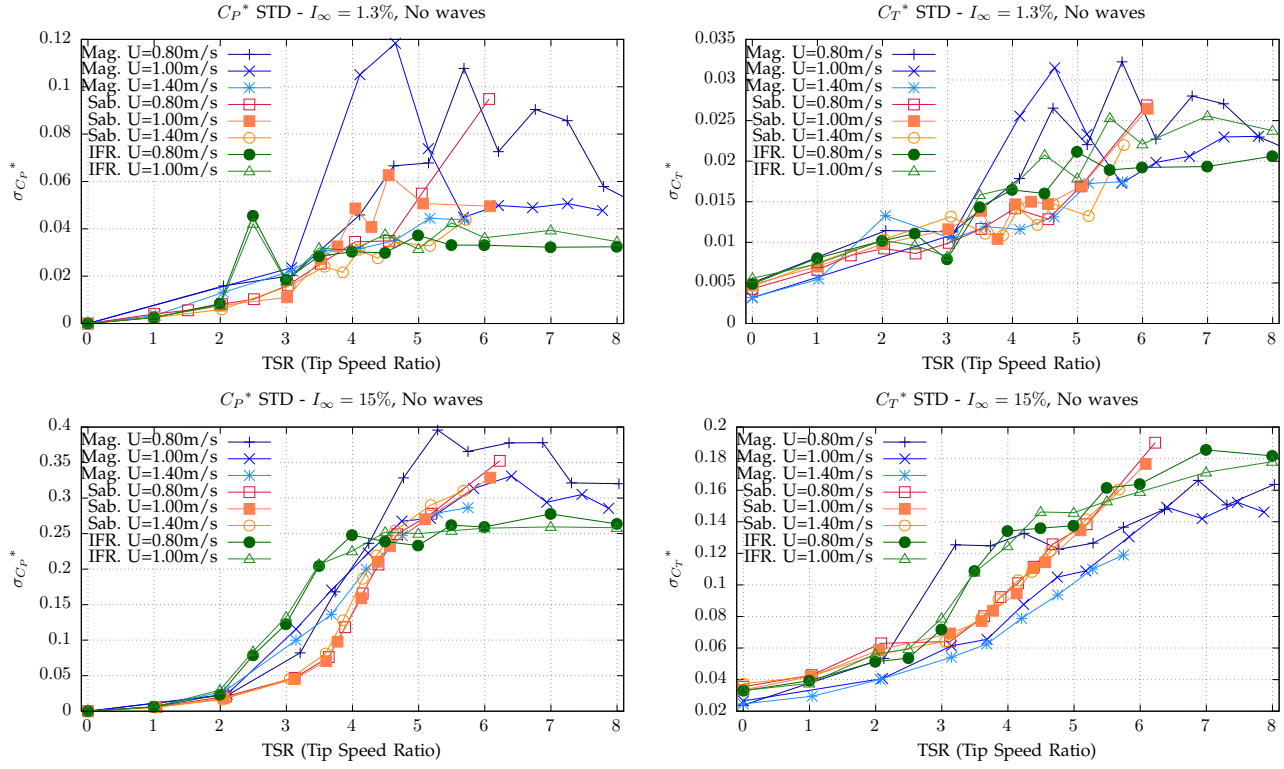

Fig. 17. Comparison of the adimensional standard deviation of Magallanes, Sabella and IFREMER turbines power and thrust coefficients for the two ambient turbulence intensity cases.

Among the three turbines tested, one turbine presented an important Reynolds effect for the lower tested velocities. Except from that, the dimensionless performance and thrust coefficients of these turbines have similar shape. Indeed, although the ambient turbulence intensity does not impact much the mean values of the power and thrust coefficients, it has an important impact on their fluctuations [2]–[4]. Differences in solidity, blade profile and blade number do not seem to have such an influence. Caution needs

to be taken with this last conclusion as all the three turbines are based on the same drive train. It may have a major influence hiding the differences due to the rotor influence. In that respect, further analysis is still required to ascertain these pieces of conclusion. Regarding the tested *current and wave* condition, no major difference was observed neither on the C_P and C_T curves nor on their fluctuations. A deeper analysis is still needed on these *current and wave* configurations in order to separate the ambient turbulence on one side, and wave on the other side, influences on the fluctuating loads. The MONITOR objective of studying fluctuating loads is crucial as this may drastically affect the fatigue of the machine, and as a result, its global manufacturing cost.

REFERENCES

[1] M. Togneri and e t Al, "Multi-model analysis of tidal turbine reliability," in *Submitted to Proceedings of the Thirteens European Wave and Tidal Energy Conference*. University of Napoli, Italy: EWTEC, 2019, pp. – , ISSN:.

[2] P. Mycek, B. Gaurier, G. Germain, G. Pinon, and E. Rivoalen, "Experimental study of the turbulence intensity effects on marine current turbines behaviour. part I: One single turbine," *Renewable Energy*, vol. 66, no. 0, pp. 729 – 746, 2014. [Online]. Available: http://www.sciencedirect.com/science/article/pii/S096014811400007X

[3] T. Blackmore, L. E. Myers, and A. S. Bahaj, "Effects of turbulence on tidal turbines: Implications to performance, blade loads, and condition monitoring," *International Journal of Marine Energy*, vol. 14, pp. 1 – 26, 2016. [Online]. Available: http://www.sciencedirect.com/science/article/pii/S2214166916300297

[4] I. Milne, A. Day, R. Sharma, and R. Flay, "The characterisation of the hydrodynamic loads on tidal turbines due to turbulence," *Renewable and Sustainable Energy Reviews*, vol. 56, pp. 851 – 864, 2016. [Online]. Available: http://www.sciencedirect.com/science/article/pii/S1364032115013623

[5] M. Togneri, M. Lewis, S. Neill, and I. Masters, "Comparison of adcp observations and 3d model simulations of turbulence at a tidal energy site," *Renewable Energy*, vol. 114, pp. 273 – 282, 2017, wave and Tidal Resource Characterization. [Online]. Available: http://www.sciencedirect.com/science/article/pii/S0960148117302537

[6] C. Faudot and O. G. Dahlhaug, "Prediction of wave loads on tidal turbine blades," *Energy Procedia*, vol. 20, pp. 116 – 133, 2012, technoport 2012 - Sharing Possibilities and 2nd Renewable Energy Research Conference (RERC2012). [Online]. Available: http://www.sciencedirect.com/science/article/pii/S1876610212007448

[7] L. Luznik, K. A. Flack, E. E. Lust, and K. Taylor, "The effect of surface waves on the performance characteristics of a model tidal turbine," *Renewable Energy*, vol. 58, pp. 108 – 114, 2013. [Online]. Available: http://www.sciencedirect.com/science/article/pii/S0960148113001316

[8] X. Guo, J. Yang, Z. Gao, T. Moan, and H. Lu, "The surface wave effects on the performance and the loading of a tidal turbine," *Ocean Engineering*, vol. 156, pp. 120 – 134, 2018. [Online]. Available: http://www.sciencedirect.com/science/article/pii/S0029801818301823

[9] P. Scheijground and A. Southal, "Advencing IEC standardization and certification for tidal energy convertors," in *Submitted to Proceedings of the Thirteens European Wave and Tidal Energy Conference*, 2019.

[10] B. Gaurier, G. Germain, J. Facq, C. Johnstone, A. Grant, A. Day, E. Nixon, F. D. Felice, and M. Costanzo, "Tidal energy round robin tests comparisons between towing tank and circulating tank results," *International Journal of Marine Energy*, vol. 12, pp. 87 – 109, 2015, special Issue on Marine Renewables Infrastructure Network. [Online]. Available: http://www.sciencedirect.com/science/article/pii/S2214166915000223

[11] B. Gaurier, G. Germain, and G. Pinon, "How to correctly measure turbulent upstream flow for marine current turbine performances evaluation?" in *Advances in Renewable Energies Offshore: Proceedings of the 3rd International Conference on Renewable Energies Offshore (RENEW 2018), October 8-10, 2018, Lisbon, Portugal. 1st Edition. Carlos Guedes Soares (Ed.). ISBN 978-1-138-58535-5. Modelling tidal currents. pp.23-30 (Taylor & Francis Group)* ., 2019.

[12] B. Gaurier, C. Carlier, G. Germain, G. Pinon, and E. Rivoalen, "Three tidal turbines in interaction: an experimental study of turbulence intensity effects on wakes and turbine performances." *Submitted to Renewable Energy*, vol. –, no. –, pp. —, 2019.

[13] B. Gaurier, S. Ordonnez, and G. Germain, "First round of marinet 2 tidal energy round robin tests: combined wave and current tests,," in *Submitted to Proceedings of the Thirteens European Wave and Tidal Energy Conference*, 2019.

[14] F. Maganga, G. Germain, J. King, G. Pinon, and E. Rivoalen, "Experimental characterisation of flow effects on marine current turbine behaviour and on its wake properties," *IET Renewable Power Generation*, vol. 4, no. 6, pp. 498–509, 2010. [Online]. Available: http://link.aip.org/link/?RPG/4/498/1

[15] O. D. Medina, F. G. Schmitt, R. Calif, G. Germain, and B. Gaurier, "Turbulence analysis and multiscale correlations between synchronized flow velocity and marine turbine power production," *Renewable Energy*, vol. 112, pp. 314 – 327, 2017. [Online]. Available: http://www.sciencedirect.com/science/article/pii/S0960148117304093

[16] K. Mccaffrey, B. Fox-Kemper, P. Hamlington, and J. Thomson, "Characterization of turbulence anisotropy, coherence, and intermittency at a prospective tidal energy site: Observational data analysis," *Renewable Energy*, vol. 76, pp. 441–453, 04 2015.

[17] B. Gaurier, P. Davies, A. Deuff, and G. Germain, "Flume tank characterization of marine current turbine blade behaviour under current and wave loading," *Renewable Energy*, vol. 59, no. 0, pp. 1 – 12, 2013. [Online]. Available: http://www.sciencedirect.com/science/article/pii/S0960148113001353

[18] EMEC, "Fall of warness data summary," European Marine Energy Center, Tech. Rep., 2016.

[19] M. Togneri, I. Masters, C. Carlier, C. Choma Bex, and G. Pinon, "Comparison of synthetic turbulence approaches for two numerical tidal turbine models," in *Proceedings of the Twelfth European Wave and Tidal Energy Conference*, A. Lewis, Ed. University College Cork, Ireland: EWTEC, Aug 27–Sep 1 2017, pp. 765 1–765 10, ISSN: 2309-1983.

[20] G. Pinon, M. F. Hurst, and E. Lukeba, "Semi-analytical estimate of energy production from a tidal turbine farm with the account of ambient turbulence," *International Journal of Marine Energy*, vol. 19, pp. 70 – 82, 2017. [Online]. Available: http://www.sciencedirect.com/science/article/pii/S2214166917300516